



14<sup>TH</sup> CANADIAN MASONRY SYMPOSIUM  
MONTREAL, CANADA  
MAY 16<sup>TH</sup> – MAY 20<sup>TH</sup>, 2021



## UNREINFORCED BRICK MASONRY FAÇADES WITH IRREGULAR OPENING LAYOUTS: MICRO VS MACRO-MODELING RESULTS

Morandini, Chiara<sup>1</sup>; Malomo, Daniele<sup>2</sup> and Penna, Andrea<sup>3</sup>

### ABSTRACT

Equivalent-frame macro-models (i.e. EFM), widely employed by both researchers and practitioners for reproducing the in-plane governed response of unreinforced brick masonry (URM) structures, typically represent an acceptable compromise between accuracy and computational cost. However, when considering URM systems with an irregular openings distribution, the definition of the effective heights and lengths of deformable components (i.e. pier and spandrel elements) still represents an open challenge. In this work, a comprehensive study is undertaken with a view to investigate the influence of the irregular openings distribution on the numerically-predicted lateral behavior of full-scale URM façades. To this end, several geometrical combinations and various degrees of irregularity are considered and subsequently idealized according to various commonly-employed EFM discretization approaches. Then, after a preliminary calibration process using experimental tests on both single piers and a full-scale URM façade, EFM results are compared with micro-modeling predictions, carried out within the framework of the Applied Element Method (AEM), where damage propagation and failure mechanisms are explicitly represented. Although, in some cases, depending on the considered EFM mesh scheme, macro and micro-models converge to similar results, non-negligible differences in initial lateral stiffness, base-shear and damage distribution were observed. Thus, a careful selection of appropriate EFM schemes is needed when performing in-plane analyses of URM systems with irregular opening layouts.

**KEYWORDS:** *unreinforced masonry; in-plane; irregular opening layouts; macro-modeling; Equivalent-Frame model; micro-modeling; Applied Element Method*

<sup>1</sup> Ph.D. Student., University of Pavia, Pavia, Italy, chiara.morandini02@universitadipavia.it

<sup>2</sup> Assistant Professor, McGill University, Montréal, Canada, daniele.malomo@mcgill.ca

<sup>3</sup> Associate Professor, University of Pavia, Pavia, Italy, andrea.penna@unipv.it

## INTRODUCTION

As shown by several investigations [1,2], the Equivalent-Frame modeling strategy (EFM) usually represents an acceptable compromise between accuracy and computational cost, often making it the preferred choice when evaluating the response of large-scale unreinforced brick masonry (URM) buildings governed by the in-plane (IP) failure modes [3,4]. Further, recent advances [5] of this method introduced the possibility of considering out-of-plane (OOP) mechanisms, thus equaling the capabilities of more refined hybrid macro-modeling approaches [6,7]. This notwithstanding, and despite the fact that the use of EFM is endorsed by many international codes, in the presence of irregular opening layouts, the identification of the effective wall height and the definition of rigid and deformable regions becomes non-unique and may lead to epistemic modeling errors. Indeed, various numerical applications e.g. [8-12], have already shown that using simplified macro-modeling strategies for analyzing irregular URM constructions can result in a significant dispersion of results.

In this work, the impact of EFM discretization on the accuracy of macro-modeling predictions is further investigated. To this end, the results obtained from calibrated EFM for a number of different irregular opening layouts, developed according to various-typically employed discretization techniques, are compared with those inferred using detailed micro-models.

## EQUIVALENT FRAME MODELING STRATEGY

In the EFM framework, masonry structures are ideally subdivided into rigid nodes and deformable portions (macroelements), Figure 1. In this work, the macroelement model initially proposed by Penna et al. [3], further improved by Bracchi et al. [13,14], and implemented in the research version of TREMURI software package [15], was considered. A given URM panel is modelled as a non-linear macroelement [16]; the latter is subdivided into three parts: a central body, where only shear deformations are allowed, and two zero-thickness spring interfaces where external axial and rotational degrees of freedom are located. A no-tension model is allotted to the spring interfaces, with a bilinear constitutive model in compression.

The shear model parameters are based on an equivalent Mohr-Coulomb criterion. They include density,  $\rho$ , Young modulus,  $E$ , shear modulus,  $G$ , compressive strength,  $f_m$ , brick tensile strength,  $f_{bt}$ ,  $G_{ct}$ , controlling the macroelement shear deformability, and  $\beta$  which influences the associated softening branch. A preliminary validation of the model, conducted using results of URM piers subjected to an IP quasi-static cyclic test and the values of the abovementioned parameters used herein, are presented in the next section. When considering complex URM systems (see Figure 1), the EFM idealization comprises the identification of both deformable (i.e. spandrels and piers) and rigid node elements.

The effective height of piers (i.e. the vertical length of the deformable portion of each macroelement) should be defined according to the expected (or assumed) crack propagation, which is affected by several factors sometimes difficult to evaluate (e.g. loading direction, presence of lintels, adjacent openings, bond pattern).

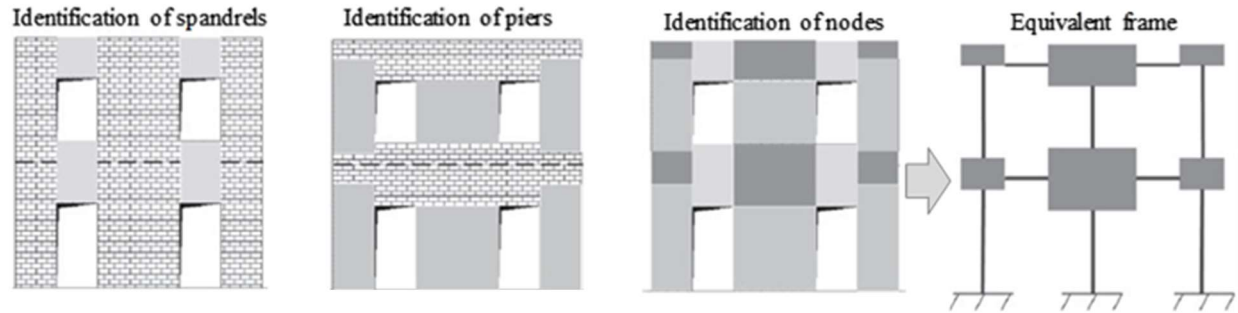


**Figure 1: EFM idealization (adapted from [15])**

In practice, this important parameter is typically determined through simplified geometrical considerations. Three commonly-employed criteria have been considered in this work and graphically represented in Figure 2, from left to right: MIN (minimum effective height), LIM (30° limited effective height) and AVG (average effective height). In more detail, the MIN criterion considers the minimum height of the masonry pier between two adjacent openings, while according to AVG, the effective height is defined by the line connecting the corners of adjacent openings. The LIM criterion limits the effective height using the AVG to a maximum inclination of 30°.

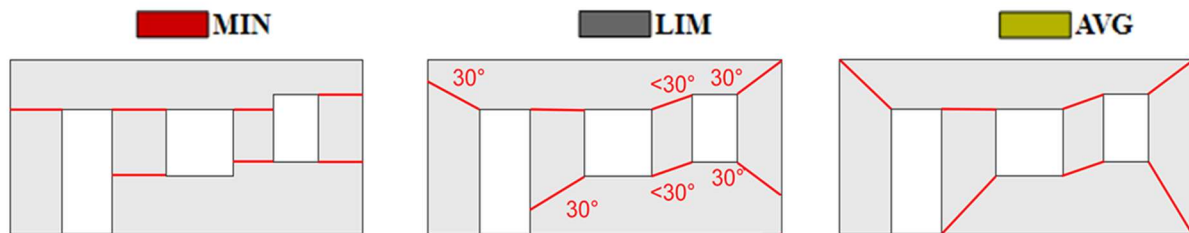


**Figure 2: Selected EFM discretization strategies**

## **APPLIED ELEMENT METHOD FOR MASONRY STRUCTURES**

As mentioned in the introduction and shown in the following sections, in this work, the micro-models results are used as a benchmark for evaluating the quality of EFM predictions, developed in the framework of the Applied Element Method (AEM) [17] and presently implemented in the commercial software Extreme Loading for Structures [18]. This recently-devised numerical approach has proven to be able to simulate adequately both quasi-static and dynamic response of URM systems of varying levels of complexity, ranging from isolated components [19] to multi-story buildings [20].

In the AEM, which can be classified as a rigid body and spring discrete model [21], a masonry element is idealized as an assembly of rigid bodies with six degrees of freedom, to which the mass of the system is allotted, and connected by zero-thickness non-linear spring interfaces, where deformation and failure occur.

With reference to the nomenclature depicted in Figure 3(a), each interface spring is characterized by a normal ( $k_{ni}$ ) and shear ( $k_{si}$ ) stiffness (equations (1)-(2)), where  $E_u$ ,  $G_u$ ,  $E_{mo}$  and  $G_{mo}$  are the unit and mortar Young's and shear moduli respectively, while  $d$  stands for the element thickness.

$$k_{ni} = \sum_{i=1}^j \left( \frac{l_u - t_{mo}}{E_u d t_u} + \frac{t_{mo}}{E_{mo} d t_u} \right)^{-1} \quad (1) \quad k_{si} = \sum_{i=1}^j \left( \frac{l_u - t_{mo}}{G_u d t_u} + \frac{t_{mo}}{G_{mo} d t_u} \right)^{-1} \quad (2)$$

$$k_{nu} = \sum_{i=1}^j \left( \frac{E_u d t_u}{l_e} \right) \quad (3) \quad k_{su} = \sum_{i=1}^j \left( \frac{G_u d t_u}{l_e} \right) \quad (4)$$

It is worth noting that the equivalent interface spring stiffnesses were obtained assuming unit and mortar springs arranged in series at an arbitrary contact point, while the unit-to-unit springs, whenever failure through brick has to be considered, can be obtained using equations (3)-(4).

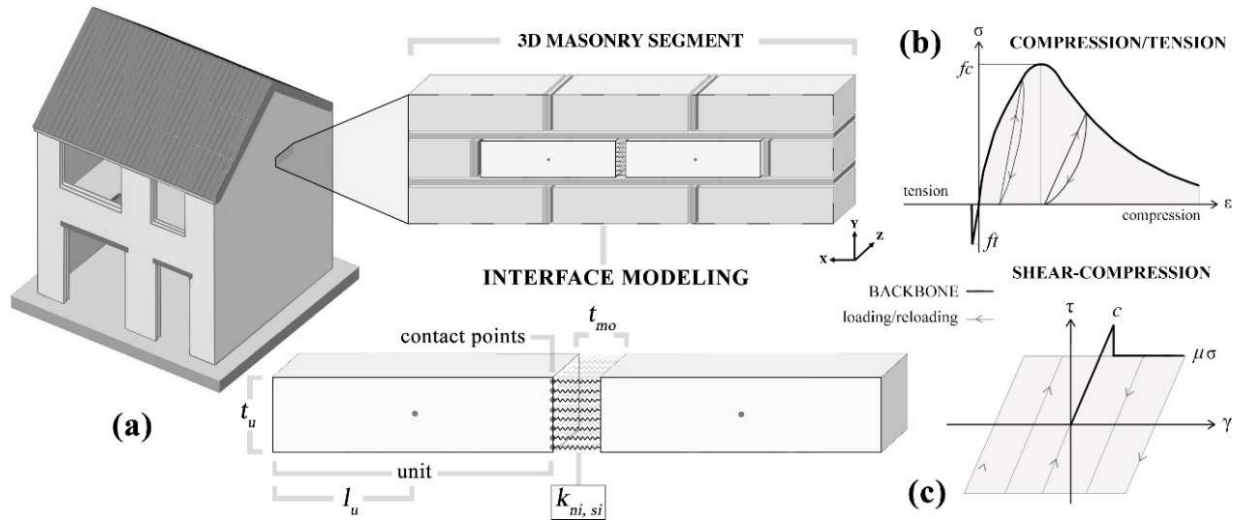


**Figure 3: (a) AEM discretization of a 3D masonry segment and normal/shear interface stiffnesses, (b) compression/tension and (c) shear-compression joint models**

While a cut-off criterion is employed for spring tensile failure, a simplified version of the elastoplastic fracture model, originally developed by El-Kashif and Maekawa [22], is commonly used for simulating the cyclic cumulative damage of masonry elements subjected to uniaxial compression (see Figure 3(b)). The hysteretic constitutive law that governs the cyclic response of shear springs is based on a Mohr-Coulomb yielding criterion, where cohesion is set to zero right after reaching the maximum shear strength, as depicted in Figure 3(c). The material model parameters are reported in Table 2, where  $c$ ,  $\mu$  and  $f_m$  are cohesion, friction coefficient, and compressive strength of brick-mortar interface, and  $f_{ut}$  is the brick tensile strength.

## PRELIMINARY CALIBRATION PROCESS

In what follows, AEM and EFM models were preliminary calibrated against experimental tests on both isolated URM piers and a full-scale URM façade subjected to quasi-static IP cyclic loading.

These were built using the same materials and construction techniques at the Ispra Joint Research Centre [23] and University of Pavia [24] (Italy), respectively.

***Simulation of the quasi-static IP cyclic response of isolated URM piers***

A squat (i.e. LW, 0.25x1x1.35m) and a slender (i.e. HW, 0.25x1x2m) masonry piers, laid in an English bond pattern, were tested at the Joint Research Centre of Ispra under quasi-static IP cyclic loading and fixed-fixed boundary conditions. A vertical surcharge of 0.6 MPa was applied through two vertical actuators to the top beam. The horizontal displacement history was applied in a quasi-static test to the top beam performing two or three cycles at each amplitude. The squat pier, LW, exhibited a brittle diagonal shear failure at 2.8 mm (corresponding to a drift of 0.2%) and a peak base shear equal to 84 kN; from this point on, recorded shear force gradually decreased until the test was stopped. The response of the slender wall, HW, was mainly governed by rocking, with only minor damage due to toe-crashing failure mechanisms and a peak base shear of 72 kN. In Figure 4, experimental vs numerical EFM and AEM hysteretic curves are reported for both the piers. Dominating failure modes, initial stiffnesses, dissipated energies as well as peak and residual horizontal forces were adequately captured by both EFM and AEM models.

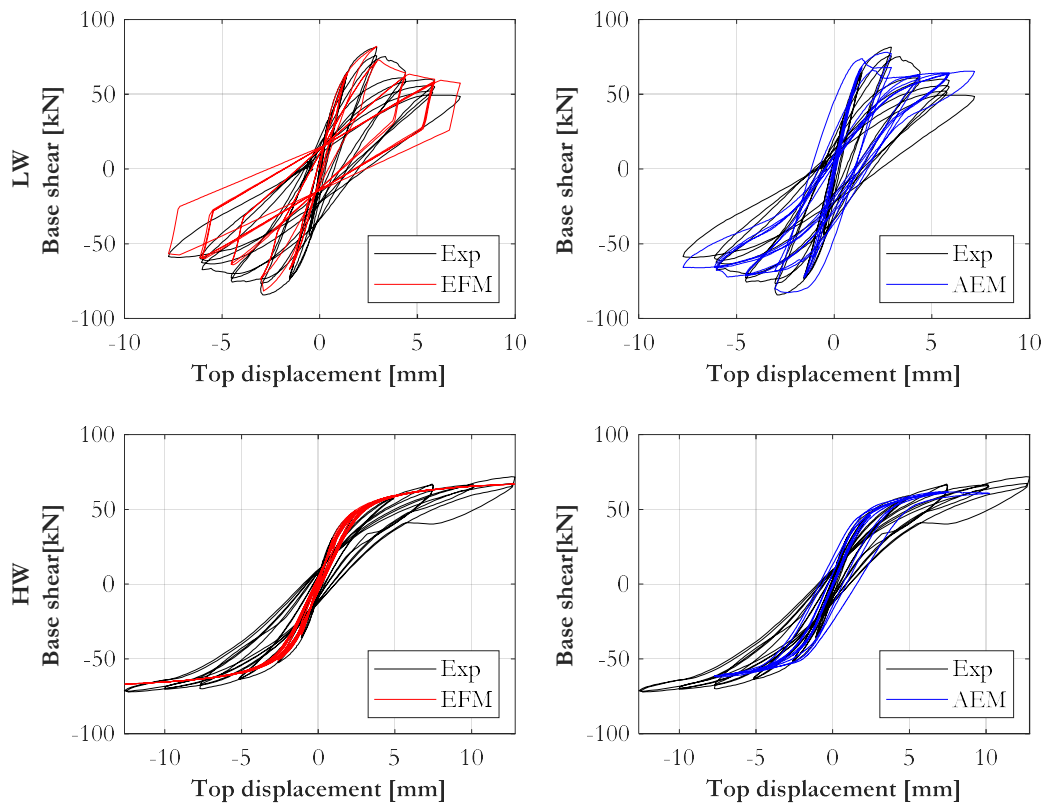


**Figure 4: Exp. vs num. force-displacement hysteresis of LW and HW obtained with the EFM (in red color, left column) and AEM (in blue color, right column) models**

***Simulation of the quasi-static IP cyclic response of a full-scale URM façade***

The full-scale prototype considered in this sub-section (hereinafter referred to as DW) consisted of a two-story URM façade (English bond pattern) with a regular opening layout and flexible

diaphragms (i.e. a series of isolated steel beams where vertical load was applied, 10 kN/m<sup>2</sup> at both 1<sup>st</sup> and 2<sup>nd</sup> floor). No out-of-plane restraints were applied. DW was tested under a quasi-static cyclic test applying horizontal forces by actuators placed at each floor level. The ratio between the horizontal forces at each level was kept constant, and the actions were applied in displacement control. To validate the EFM and AEM numerical models, two monotonic quasi-static analyses were performed, and inferred results compared with the experimental backbone curves. Material properties adopted are reported in Table 1 and Table 2.

**Table 1: Calibrated material properties of piers for MIN, AVG and LIM criteria**

	$\rho$ [kg/m <sup>3</sup> ]	E [MPa]	G [MPa]	$f_m$ [MPa]	$f_{bt}$ [MPa]	$G_{ct}$ [-]	$\beta$ [-]
<b>MIN</b>	1800	1570	600	6.20	0.80	1.90	0.30
<b>LIM</b>	1800	2000	1000	6.20	0.83	3.30	0.25
<b>AVG</b>	1800	2000	1000	6.20	0.83	4.00	0.25

**Table 2: Calibrated material properties of AEM model**

$\rho$ [kg/m <sup>3</sup> ]	$E_{mo}$ [MPa]	$G_{mo}$ [MPa]	$E_u$ [MPa]	$G_u$ [MPa]	$f_m$ [MPa]	$c$ [MPa]	$f_{ut}$ [MPa]	$\mu$
1800	1324	530	4680	1872	6.20	0.23	1.30	0.80

As shown in Figure 5, good agreement was found between numerical and experimental results in terms of initial lateral stiffness, peak and residual base shear. The difference between numerical curves and experimental backbone for initial stiffness is around 15%, while minor differences were found with respect to the peak base shear (8%), although the peak was reached at different drift. In the AEM, the damage is shown in terms of crack propagation, assuming that cracks occur when the tensile failure on the interfaces springs is reached. In the EFM, the shear damage parameter  $\alpha > 1$  represents the attainment of the maximum shear capacity of the macroelement. The experimental damage, Figure 6 (a), is reported as a benchmark and compared with the AEM crack pattern, Figure 6 (b), and EFM, Figure 6 (c), damage.

### **INFLUENCE OF EFM DISCRETIZATION ON PREDICTED RESPONSE**

The modeling assumptions validated in the previous sections were herein adopted to analyze a set of façades with different irregular openings configurations (Figure 7), generated taking as a reference calibrated material properties, geometry and construction details implemented in the DW models. Then, quasi-static IP monotonic analyses were performed to compare initial lateral stiffnesses and force-displacement relationships predicted by the selected EFM discretizations with those inferred using the more refined AEM models. Figure 8 shows the EFM results in terms of difference with respect to the AEM counterparts, expressed in percentage form.

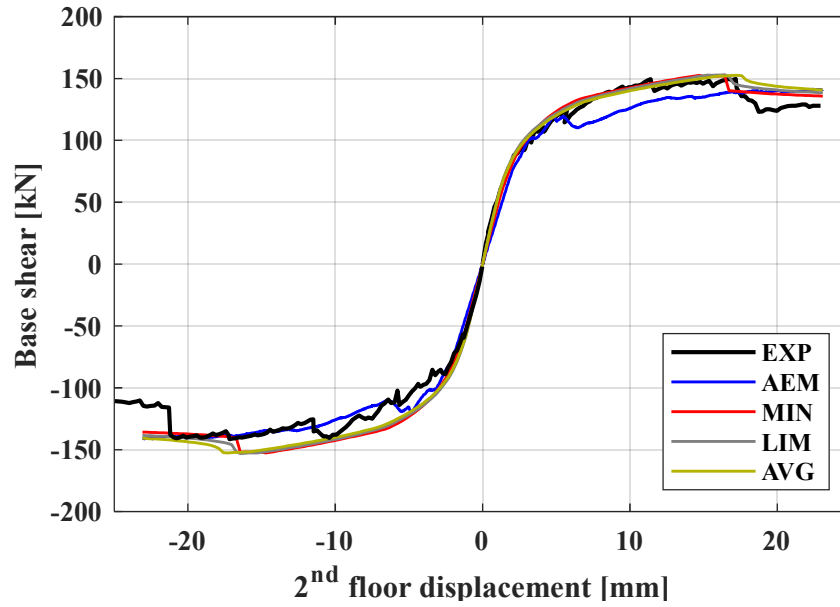


Figure 5: Comparison between exp. backbone curve and num. IP monotonic curves

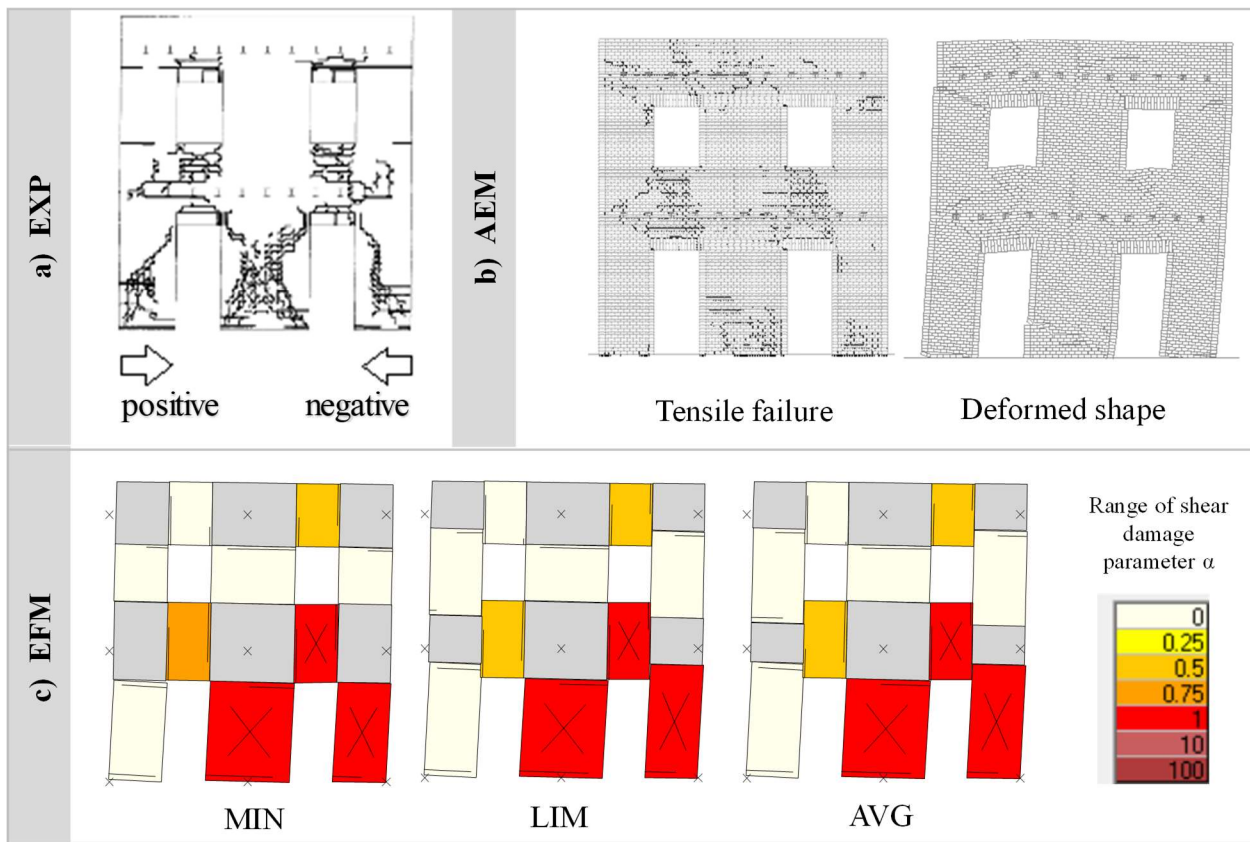


Figure 6: a) Experimental, b) AEM and c) EFM damage

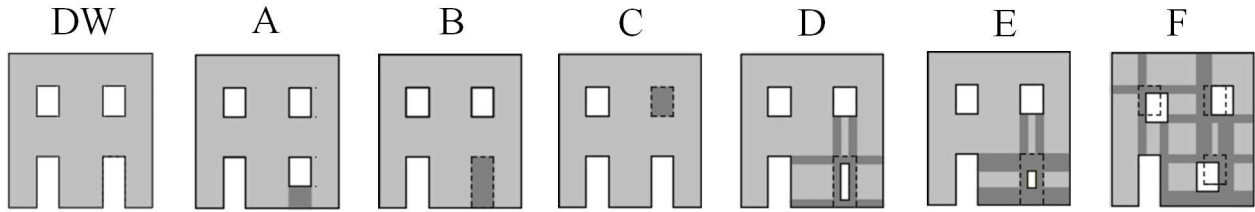


Figure 7: Considered openings distributions

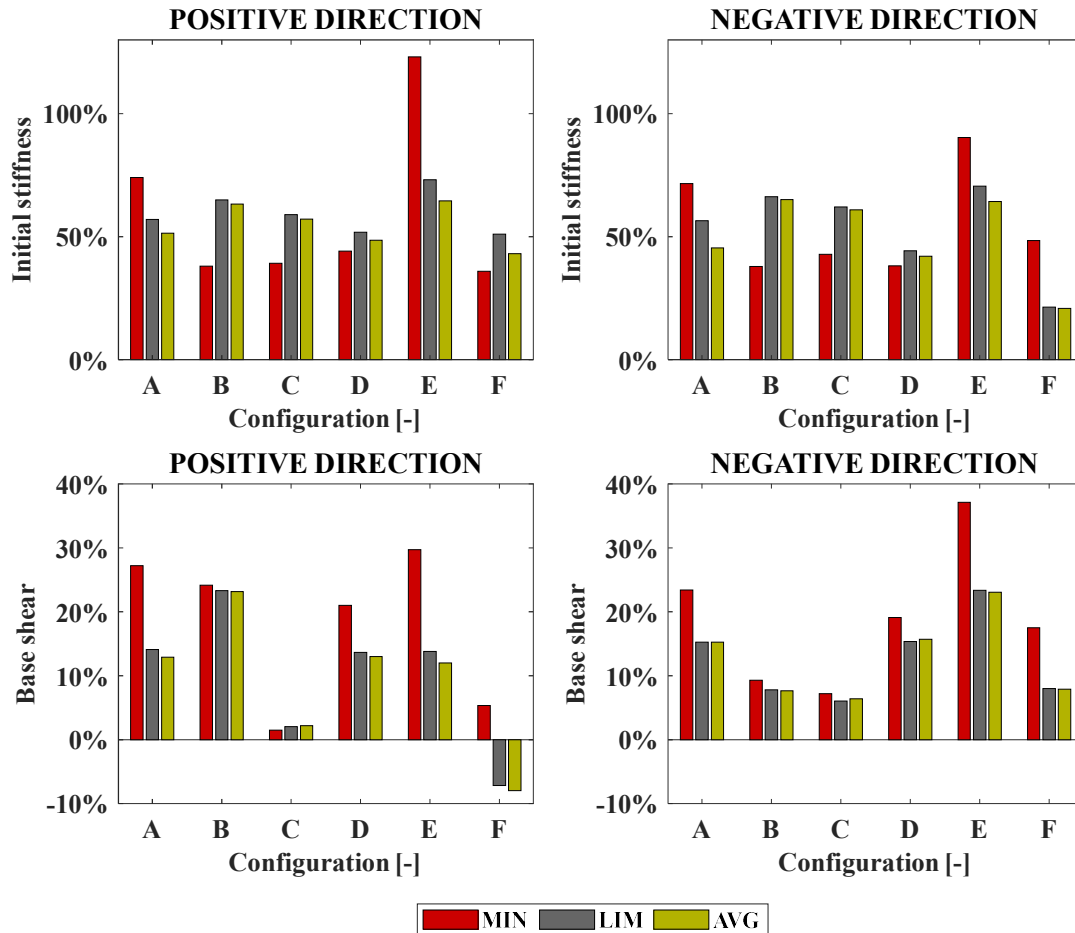


Figure 8: Parametric analysis results in terms of initial lateral stiffness and peak base shear differences with respect to the AEM counterparts, here expressed in percentage form.

The deformed shape and crack patterns predicted by the AEM models (not shown here due to space constraints) indicate that usually damage was concentrated in specific and recurring areas of the façades - while some others only suffered minor damage, and thus work as rigid elements. This latter aspect is encouraging and suggests that even when irregular openings distributions are considered it might be still possible to apply EFM modeling strategies. In general, EFM models predicted higher base shear capacities and initial stiffnesses. It is worth mentioning that, as already



noted by Malomo et al. [8], the discrete model usually tends to predict lower initial stiffness than EFM models, which is in line with what has been observed in this study.

Regarding the selected EFM discretization criteria, they often led to the definition of deformable pier and spandrel elements with different aspect ratios, which resulted in different predicted IP responses, sometimes significantly differing from the AEM ones ( +20 to +120% initial stiffness and up to 40% base shear, see Figure 8). The major dispersion in terms of initial stiffness and peak base shear was found when the geometric irregularity is located at the ground floor, as the piers at this level essentially governed the overall IP response, as it happened experimentally for DW. This notwithstanding, non-negligible differences between AEM and EFM models were also found in configuration C, where the irregularity is located at the first level. These differences were probably due to the fact that EFM regions, assumed fully rigid according to MIN, AVG and LIM models, exhibited instead damage in the AEM counterparts.

In general, MIN discretization generated larger rigid node regions comparing to AVG, LIM and to the uncracked regions predicted by AEM models, leading to a stiffer response and higher peak base shear, which substantially confirmed similar previous investigations [11,12]. AVG and LIM-based EFM models often converged on similar results instead, usually close to those of the AEM ones. Moreover, when small openings are considered (e.g. configuration E), cracks propagation in AEM suggests the activation of a single strut only, as was also noted by Camilletti [25]. This is different from EFM models, where two deformable portions surrounding the small opening are considered and consequently leads to different predictions of the façade response by the two modeling approaches.

## **CONCLUSIONS**

The application of Equivalent Frame macro-models (EFM) to the seismic assessment of the in-plane governed behavior of URM buildings usually produces accurate results in a reasonable timeframe. For this reason, they are widely employed by both practitioners and researchers and endorsed by several international codes. The identification of the frame elements, namely (spandrels, piers and rigid nodes), can be challenging in the presence of irregular openings distributions, and their inaccurate definition might lead to modeling errors, thus affecting the quality of numerical predictions. This work evaluates the influence of EFM discretization on modeling accuracy; three different commonly-employed EFM discretization criteria (i.e. MIN, LIM, AVG) based on simple geometrical considerations were selected, and their effectiveness scrutinized through a comprehensive study which comprised several irregular opening layouts. This also included comparisons against more detailed micro-models, using the Applied Element Method (AEM).

EFM and AEM models were preliminarily calibrated against quasi-static in-plane cyclic tests on two isolated components, with markedly different aspect ratios, and a full-scale façade with flexible diaphragms. Given the encouraging results obtained and the good agreement found with

respect to the experimental counterparts, the modeling assumptions adopted in the abovementioned modeling exercises were also implemented in the models used in the parametric study.

Regarding the latter, it is worth noting that non-negligible differences were found between the considered EFM discretization approaches and the AEM micro-models, both in terms of initial lateral stiffness (from 20% to 120%) and peak base shear (up to 40%). Nonetheless, the outcomes of this study indicate that a careful evaluation of the EFM layout may reduce these differences. The investigation showed that, even with irregular openings distribution, it was possible to identify in the AEM models recurring uncracked regions and other portions of the structure where damage was usually concentrated. Interesting avenues for further research include considering a broader number of façade geometries, including configurations with more marked misalignments and/or smaller openings. This will allow the development of a generic and readily-applicable rule, which will be valid even when considering irregular opening layouts.

## ACKNOWLEDGEMENTS

This work was conducted within the framework of the ReLUIS-DPC WP10 Project 2019-2021 funded by the Italian Department of Civil Protection, whose support is gratefully acknowledged.

## REFERENCES

- [1] Sangirardi, M., Liberatore, D. and Addessi, D. (2019). “Equivalent Frame modelling of masonry walls based on plasticity and damage.” *Int. J. Archit. Herit.*, 13(7), 1098–109.
- [2] Kallioras, S., Graziotti, F. and Penna, A. (2019). “Numerical assessment of the dynamic response of a URM terraced house exposed to induced seismicity.” *Bull. Earthq. Eng.*, 17(3), 1521–1552.
- [3] Penna, A., Lagomarsino, S. and Galasco, A. (2014). “A nonlinear macroelement model for the seismic analysis of masonry buildings.” *Earthq. Eng. Struct. Dyn.*, 43, 159–179.
- [4] Raka, E., Spacone, E., Sepe, V. and Camata, G. (2015) “Advanced frame element for seismic analysis of masonry structures : model formulation and validation.” *Earthq. Eng. Struct. Dyn.*, 44, 2489–2506.
- [5] Vanin, F., Penna, A. and Beyer, K. (2020) “A three-dimensional macroelement for modelling the in-plane and out-of-plane response of masonry walls.” *Earthq. Eng. Struct. Dyn.*, 49, 1365–1387.
- [6] Pantò, B., Cannizzaro, F., Calì, I. and Lourenço, P.B. (2017). “Numerical and experimental validation of a 3D macro-model for the in-plane and out-of-plane behavior of unreinforced masonry walls.” *Int. J. Archit. Herit.*, 11(7), 946–964.
- [7] Malomo, D. and DeJong, M.J. (2021). “A Macro-Distinct Element Model (M-DEM) for simulating the in-plane cyclic behavior of URM structures.” *Eng. Struct.*, 227, 111428.
- [8] Berti, M., Salvatori, L., Orlando, M. and Spinelli, P. (2017). “Unreinforced masonry walls with irregular opening layouts: reliability of equivalent-frame modelling for seismic vulnerability assessment.” *Bull. Earthq. Eng.*, 15(3), 1213–1239.
- [9] Parisi, F. and Augenti, N. (2013). “Seismic capacity of irregular unreinforced masonry walls with openings Fulvio.” *Earthq. Eng. Struct. Dyn.*, 42, 101–121.

- [10] Quagliarini, E., Maracchini, G. and Clementi, F. (2017). “Uses and limits of the Equivalent Frame Model on existing unreinforced masonry buildings for assessing their seismic risk: A review.” *J. Build. Eng.*, 10, 166–82.
- [11] Malomo, D., Morandini, C., Penna, A. and DeJong, M.J. (2019). “Assessing the reliability of the equivalent-frame idealisation of URM façades with irregular opening layouts by comparison with the discrete micro-models.” *Proc. SECED Conference*, Greenwich, London
- [12] Morandini, C., Caserini, M., Malomo, D., Penna, A. and DeJong, M.J. (2019). “Equivalent-Frame models idealisation of laterally-loaded URM facades with irregular opening distributions.” *Proc. 18th ANIDIS Conference*, Ascoli Piceno, Italy.
- [13] Bracchi, S., Galasco, A. and Penna A. (2021) “A novel macroelement model for the nonlinear analysis of masonry buildings. Part 1: Axial and flexural behavior.” *Earthq. Eng. Struct. Dyn.*, 1-20. DOI: 10.1002/eqe.3445
- [14] Bracchi, S. and Penna, A. (2021) “A novel macroelement model for the nonlinear analysis of masonry buildings. Part 2: Shear behavior.” *Earthq. Eng. Struct. Dyn.* 1–21. DOI: 10.1002/eqe.3444
- [15] Lagomarsino, S., Penna, A., Galasco, A. and Cattari, S. (2013). “TREMURI program: An equivalent frame model for the nonlinear seismic analysis of masonry buildings.” *Eng. Struct.*, 56, 1787–1799.
- [16] Gambarotta, L. and Lagomarsino, S. (1997). “Damage models for the seismic response of brick masonry shear walls. Part II: the continuum model and its applications.” *Earthq. Eng. Struct. Dyn.*, 26(4), 441–462.
- [17] Meguro, K. and Tagel-Din, H. (2000). “Applied Element Method for structural analysis: Theory and application for linear materials.” *Struct. Eng. Earthq. Eng.*, 17(1), 21s-35.s.
- [18] Applied Science International LLC. (2018). *Extreme Loading for Structures*.
- [19] Malomo, D., Pinho, R. and Penna, A. (2020). “Numerical modelling of the out-of-plane response of full-scale brick masonry prototypes subjected to incremental dynamic shake-table tests.” *Eng. Struct.*, 209, 110298.
- [20] Karbassi, A. and Nollet, M-J. (2013). “Performance-based seismic vulnerability evaluation of masonry buildings using applied element method in a nonlinear dynamic-based analytical procedure.” *Earthq. Spectra*, 29, 399–426.
- [21] D’Altri, A.M., Sarhosis, V., Milani, G. et al. (2020). “Modeling strategies for the computational analysis of unreinforced masonry structures: Review and classification.” *Arch. Computat. Methods. Eng.*, 27, 1153–1185.
- [22] El-Kashif, K.F. and Maekawa, K. (2004). “Time-dependent nonlinearity of compression softening in concrete.” *J. Adv. Concr. Technol.*, 2(2), 233–247.
- [23] Anthoine, A., Magonette, G. and Magenes, G. (1995). “Shear-compression testing and analysis of brick masonry walls.” *Proc. 10th European Conference on Earthquake Engineering*, Vienna, Austria.
- [24] Magenes, G., Kingsley, G.R. and Calvi, G.M. (1995). “Seismic testing of a full-scale, two-story masonry building: test procedure and measured experimental response.” *Consiglio nazionale delle ricerche, Gruppo nazionale per la Difesa dai terremoti*, Pavia, Italy.
- [25] Camilletti, D., Cattari, S. and Lagomarsino, S. (2018). “In plane seismic response of Irregular URM walls through Equivalent Frame and Finite Element Models.” *Proc. 16th European Conference on Earthquake Engineering*, Thessaloniki, Greece.